Hardware-in-the-loop testing of intelligent electronic device for innovative UFLS protection

R. Ilievska, R Mihalic, U. Rudez
University of Ljubljana
Faculty of Electrical Engineering
Trzaska 25, 1000 Ljubljana, Slovenia
rajne.ilievska@fe.uni-lj.si

E. Kushnikov
Relematika Ltd.
Prospekt Yakovleva 1
428020 Cheboksary, Russia
kushnikov_ea@relematika.ru

J. Zakonjsek
Relarte Ltd.
Ulica Pod gozdom 11
4264 Bohinjska Bistrica, Slovenia
janez.zakonjsek@relarte.com

Abstract

In recent years electric power systems are subject to drastic changes. This affects frequency stability due to decreasing trend of system inertia. For securing stable system operation in the future, it is of great importance to make existing/conventional under-frequency load shedding protection schemes more adaptable and situationally aware during various volatile conditions. This paper provides the results of hardware-in-the-loop testing of an intelligent electronic device equipped with innovative load shedding algorithm. The results obtained from applying real-time digital simulations demonstrate that the innovation is robust, efficient and offers a very useful way of utilizing rate-of-change-of-frequency for under-frequency load shedding purposes.

Index Terms

hardware-in-the-loop testing, real-time simulation, under-frequency load shedding protection, rate-of-change of frequency, intelligent electronic device

I. Introduction

Nowadays electric power systems (EPSs) are evolving in the trend of the smart grid, changing the classical EPS operation paradigm. The massive increase of penetration of renewable generation units, more power electronics and highly variable power flows negatively affect the frequency stability. Having in mind that the replacement of the conventional generation power plants with converter-interfaced generation units decreases the system inertia, securing the operation of the EPS becomes a challenge. Previously, due to the inertia of the synchronous generators the frequency was less sensitive to active-power incidents. As the inertia decreases, the frequency becomes more vulnerable and more prone to deviations even with relatively low active-power imbalance. Under-frequency load shedding (UFLS) protection schemes are responsible to stabilize the frequency and prevent system collapse when the primary control mechanisms are not capable to achieve that. Most of the UFLS protection in practice relies on conventional approaches, which become inappropriate from the perspective of modern EPS, since they lack flexibility in their operation. The conventional UFLS protection schemes use a single criterion tripping functionality, i.e. the frequency value $f(t)$ that is compared to a frequency threshold f_{thr}. When the threshold is violated as a result of a disturbance event, a tripping signal is generated by the under-frequency relay disconnecting a portion of the load specified for each shedding stage. Due to the newly arisen conditions in the EPSs, much faster frequency changes will be encountered and power re-balancing should be more precise accordingly to the severity of the incident. Therefore, it is of great importance that UFLS protection schemes become adaptable to various operating conditions. However, this is not possible using a single criterion.

The innovative UFLS proposed in [1] uses double criteria tripping functionality. The first criterion is identical to the conventional type UFLS, i.e. the frequency $f(t)$. The second criterion is the variable called frequency-stability margin $M(t)$. In its essence, a crucial variable for the innovative UFLS is the rate-of-change of frequency $ROCOF(t)$. In the research field, the potential of the $ROCOF$ has been identified for improvement in UFLS protection ([1]–[4]). However, its practical application faces challenges, due to the concern of the reliability of $ROCOF(t)$ measurement. In spite of that, ref. [5] proves that the innovative UFLS technology is feasible and robust in practical applications.

This paper presents the results from hardware-in-the-loop (HIL) testing of an intelligent electronic device (IED) TOR 300 EA 525, which performs the innovative UFLS algorithm. The IED, developed and produced by Relematika Ltd., was provided to

University of Ljubljana for HIL testing. HIL testing involved the real-time digital simulator RTDS and the physical IED. The focus of the testing was observing how the algorithm affected the UFLS in overall, from system-integrity protection scheme (SIPS) perspective. Section II gives the basics of the innovative UFLS. In section III, hardware-in-the-loop setup is presented, whereas section IV evaluates the testing results. Finally, section V concludes the paper.

II. Innovative UFLS basics

In case of an extreme incident in EPS when a larger power mismatch occurs, frequency deviations are fast and UFLS protection schemes intervene to prevent the frequency from reaching critical values. However, conventional UFLS, which are dependent on a single criterion, are becoming out-of-date and may not disconnect the right amount of load [1]. In order to make the UFLS protection scheme more adaptable, a second criterion is introduced - the frequency stability margin *M(t)*. Frequency-stability margin is a time-related variable, that is to say it estimates the time before the frequency stability limit f_{LIM} is violated. This variable is calculated in real-time from the frequency measurement *f(t)* and its corresponding rate-of-change of frequency *ROCOF(t)*:

$$M(t) = \frac{f_{LIM} - f(t)}{ROCOF(t)} \qquad (1)$$

A large value of *M(t)* indicates that the frequency is almost stable, while smaller values od *M*(*t*) indicate that frequency is dropping quickly and a specific UFLS stage may be activated. For each UFLS stage, additional M_{thr} thresholds are defined. The innovative UFLS protection is activated once both thresholds f_{thr} and M_{thr} are violated simultaneously. The relation between *f(t)* and *M(t)* is represented in terms of a *f(t)-M(t)* diagram as shown in Figure *1*.

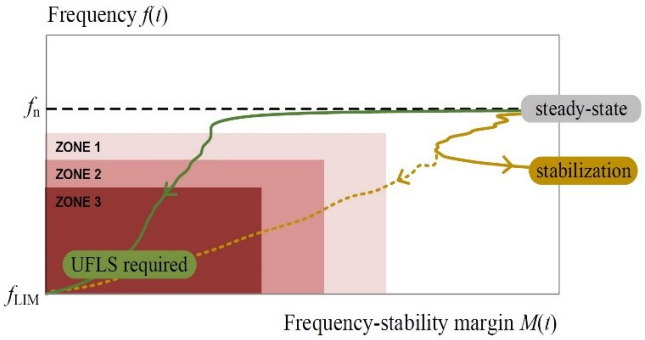

Figure 1. Representation of f(t)-M(t) diagram

The green and the yellow curves in Figure *1* represent two possible trajectories in *f(t)-M(t)* diagram after two different disturbances in the EPS, respectively. When a disturbance is moderate, the yellow curve shows that there is still enough time to stabilize the frequency by primary control mechanisms, before an UFLS is activated. On the other hand, the green curve depicts an extreme scenario when frequency drops very fast. Consequently, an immediate activation of UFLS is needed. In this kind of diagram, we can define protection zones represented with shaded areas defined by the f_{thr} and M_{thr}, correspondingly. *These f-M zones can be considered as an analogy to distance protection zones*. Each zone is related to a specific UFLS stage. The implementation logic is an upgrade of the existing/conventional UFLS protection scheme. Alongside the frequency *f(t)* input, *ROCOF(t)* is the one making a significant contribution. Both input signals go through filtering process and are used for the calculation of the frequency-stability margin *M*(*t*). Next, *f(t)* and *M(t)* are compared to their threshold values and if both are violated simultaneously, a trip signal is generated by the relay.

Our testing was based on the conventional UFLS used in Slovenia, which includes six UFLS stages, each defined with a corresponding frequency threshold. A total capacity sum of these stages is 55% of load decrease as suggested in [6]. The innovative UFLS additionally includes the frequency stability margin thresholds for each UFLS stage. TABLE 1 gives the specifics for the innovative UFLS settings, applied during testing.

TABLE 1. UFLS settings

UFLS stage number	f_{thr}[Hz]	M_{thr}[s]	Load shed [%]
1.	49.0	11.0	10
2.	48.8	9.0	10
3.	48.6	7.0	10
4.	48.4	5.0	10
5.	48.2	4.0	10
6.	48.1	3.0	5

III. Experimental hardware-in-the-loop setup

Real time digital simulator RTDS allows physical equipment and algorithms to be tested by means of a HIL prior their deployment in the real EPS. The external device, that can be any IED in general, is interfaced in a closed loop to a simulated testing environment, which runs in real time, giving insight of the IED's performance as it would be operating in the real EPS. In this way, the protection relay itself together with the protection scheme to which it contributes, are subjected literally to any kind of operating conditions, allowing the user to get familiar with their behavior and performance, as well as the response of the EPS.

Figure 2 gives the HIL setup assembled in our laboratory. It consists of RTDS simulator, which runs the simulation model, amplifier to scale-up the low level signals generated by RTDS, protection relay TOR 300 EA 525 incorporating the innovative UFLS algorithm and of course, power supply for the relay and a personal computer with RSCAD software package representing the human-machine interface. The communication between RTDS and the external device under test is achieved by means of specialized GTAO analogue output card and GTFPI digital input card.

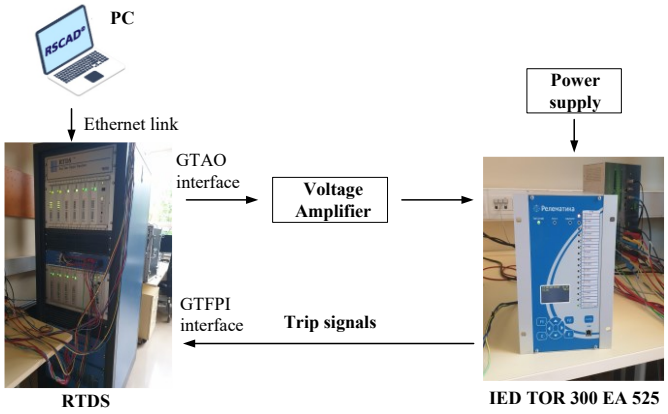

Figure 2. Hardware-in-the-loop setup

A. Intelligent electronic device – TOR 300 EA 525

The IED under test, i.e. the protection relay TOR 300 EA 525, incorporates the innovative UFLS algorithm, allowing six UFLS stages that generate trip signals. However, only the first three stages are supplied to a binary output on the IED terminals, while stages 4 to 6 do not have this possibility. The IED receives three-phase voltage signal from a specified bus in the simulation model, appropriately amplified. The frequency *f(t)* and *ROCOF(t)* are then internally calculated/estimated and used by the UFLS algorithm.

B. Software replica relay model

For our testing, we created software replica relay model within the *C-builder* module in RSCAD. The model allows six output UFLS stages and offers the user a possibility to specify the settings for the UFLS. Designated input signals for the replica are *f(t)* and *ROCOF(t)* measurements from a software model of a phasor measurement unit (PMU) included in the RSCAD model library. Both measurements were set to 200 Hz reporting rate. The software replica controls the circuit breakers for stages 4 to 6 on the bus where the physical relay is interfaced. Nevertheless, we observed all six stages outputs from the replica in order to compare the results, as it is demonstrated in Figure *3*. Moreover, since we had only one physical device, the software replica was used to control the rest of the loads in the EPS, which were considered to be part of the UFLS protection scheme.

C. IEEE 9-bus system test model

We performed the testing in two independent testing environments. The first one was the IEEE 9-bus EPS shown in Figure 4. The original benchmark IEEE 9-bus system consists of three synchronous generators with their control components and step-up transformers, six transmission lines and three equivalent loads, whose specifics can be found in [7]. The equivalent inertia of the system is H_{eq} = 5.824 s. In order to perform testing for UFLS purposes, we applied the modifications suggested in [5]. We added the UFLS relays as presented in Figure 4: the physical IED controlled first three portions of Load 5 on bus 5, while the software replica controlled the remaining three portions. Each load portion represents an individual UFLS stage.

D. Microgrid test model

The second EPS model was a low inertia microgrid system with distributed energy resources (DER), namely a diesel generator (DG) and two photovoltaic (PV) arrays. The inertia of the diesel generator, representing the only rotating generating facility with inherent inertia, is H_{eq} = 3 s. Figure 5 present the microgrid test system used in the simulations. The microgrid can operate in grid-connected or islanded operation mode by connecting/disconnecting the power source. Three of the loads were considered

for UFLS. This model was used specifically to test the UFLS in low-inertia conditions. In such case, due to the low inertia, frequency changes fast, consequently *ROCOF(t)* has higher values. Moreover, *ROCOF(t)* is calculated as a time derivative of the frequency, which leads to amplification of the noise contained in the frequency measurement. Therefore, the main concern was whether *ROCOF(t)* measurement is reliable for the operation of the UFLS protection especially under low-inertia conditions and in the presence of converters.

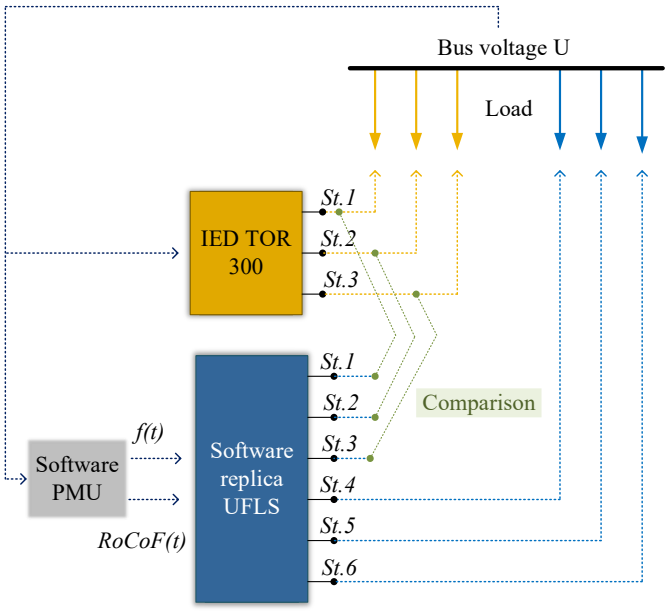

Figure 3. Monitoring software replica outputs for the evaluation of IED TOR 300 EA 525

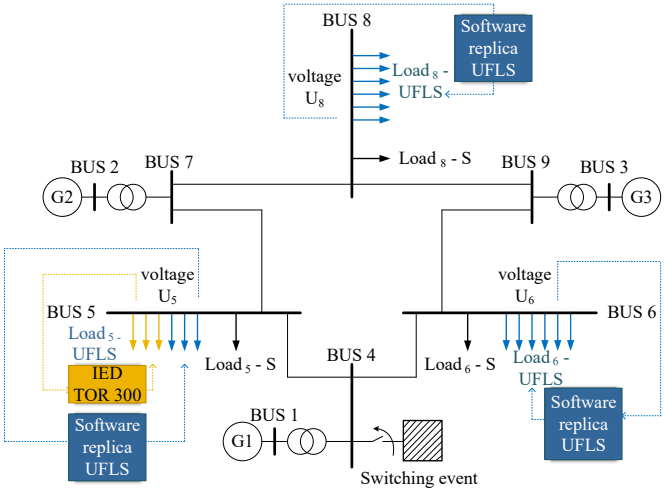

Figure 4. Modified IEEE 9-bus test system

IV. Simulation results

A. IEEE 9-bus system

In order to test the IED performance with the innovative UFLS functionality we performed a simulation set that consists of 33 simulation cases in which different power imbalances were simulated during the transition into island operation. In each simulation case, we gradually decreased the generators' output prior the main incident by 2% per case. Therefore, in every consecutive case the contribution of a power source in normal operation conditions was increased, causing larger frequency decay when the switching event was initiated and island was formed. In continuation Figure *6* and Figure *7* show the results of two simulation cases, represented in *f(t)-M(t)* diagrams. In simulation case 11 (Figure *6*), the output power of the generators was reduced by 22%, while in simulation case 25 (Figure *7*) was 50% less than the initial power output.

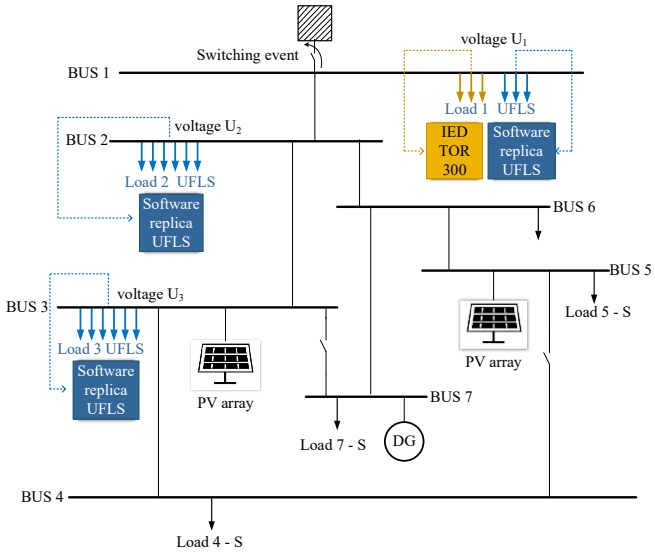

Figure 5. Microgrid test system

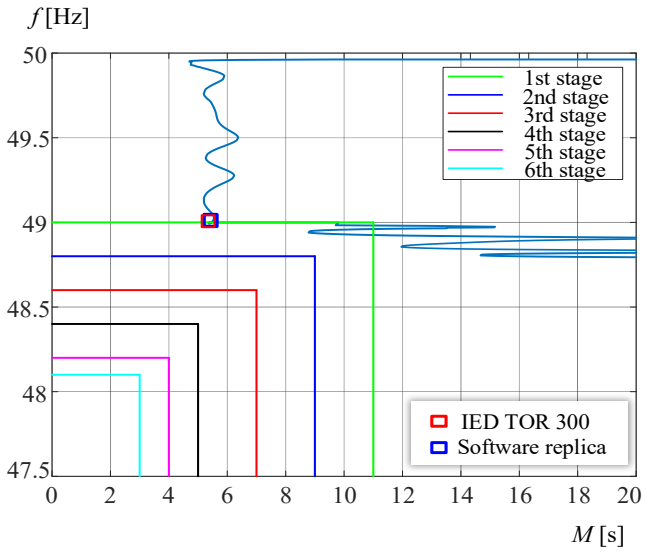

Figure 6. Simulation case 11, IEEE 9-bus system

In Figure *6* it can be noticed that the frequency criterion for activation of the 2nd UFLS stage was met, but the frequency-stability margin criterion was not, which resulted in avoiding unnecessary load disconnections. We present a similar situation in Figure *7*, where activation of four UFLS stages were required for attaining frequency stabilization.

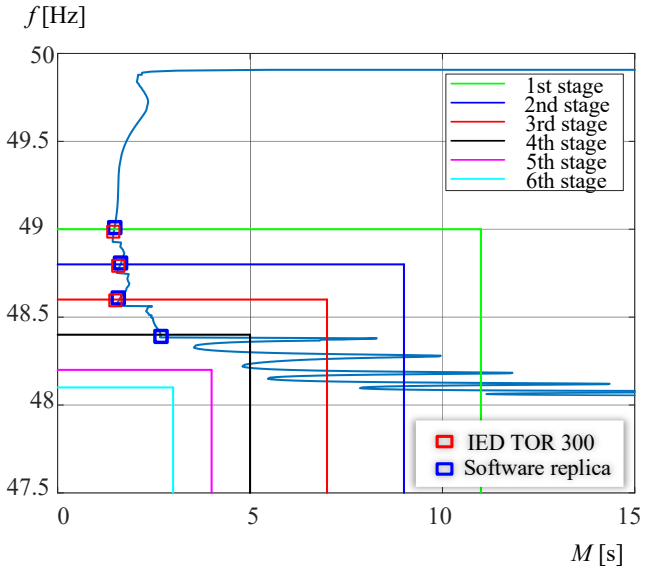

Figure 7. Simulation case 25, IEEE 9-bus system

B. *Microgrid results*

For the microgrid model, we performed a simulation set with different power imbalance conditions resulting from decreasing the power output from the diesel generator by 2% in each successive case. The results show that the microgrid model is much more prone to fast frequency decays, i.e. extreme *ROCOF* values compared to the IEEE 9-bus model due to the lower system inertia. This means that it requires much faster UFLS activation. Figure *8* and Figure *9* depict the *f(t)-M(t)* diagrams from simulation cases 10 and 23, respectively.

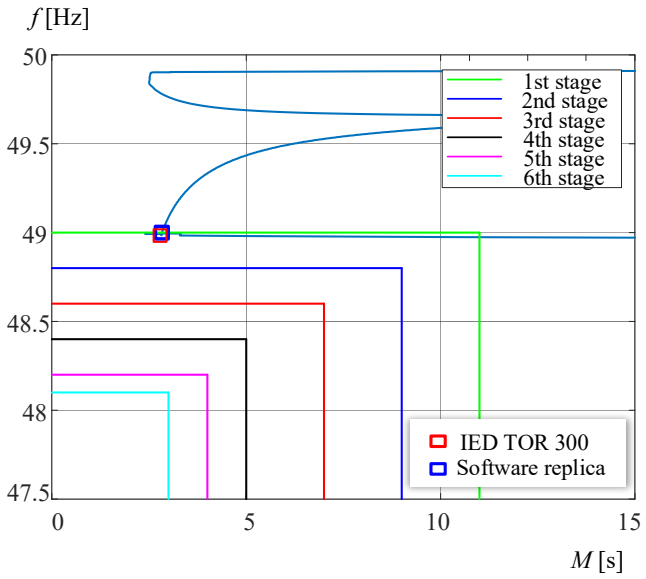

Figure 8. Simulation case 10, microgrid

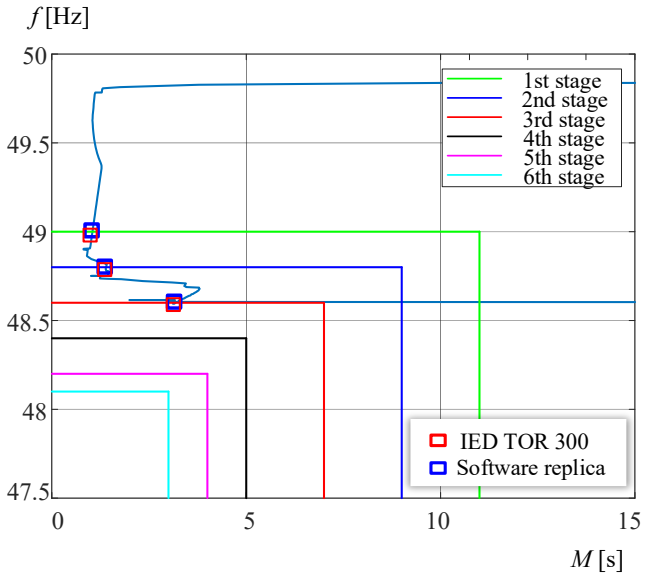

Figure 9 Simulation case 23, microgrid

V. Conclusion

In this paper we presented the results obtained from the HIL testing of IED TOR 300 EA 525 equipped with innovative UFLS algorithm. Using the RTDS simulator, we modelled two testing environments, the IEEE 9 bus test system as one of the most widely used UFLS testing model and a microgrid test model as a representative of a low inertia system with converter-based generation. The results demonstrate that the innovative UFLS is feasible, robust and efficient. *ROCOF(t)* was successfully applied for real-time calculation of the frequency-stability margin *M(t)* without causing any stability issues to the IED. The existing IED single criterion tripping functionality was successfully expanded into a double criteria tripping functionality, successfully merging frequency-stability margin *M(t)* with frequency measurement *f(t)*. According to the results obtained from the IEEE 9-bus test system, the innovative UFLS functionality kept more load supplied while at the same time achieving frequency stabilization as required for system operation purposes. As for the microgrid model, in high *ROCOF(t)* conditions the innovative UFLS acts fast as the conventional UFLS, posing no risk for system security.

From our research another very important conclusion can be drawn which will lead our future work. A presented two-criteria UFLS can be considered as a buffer against any kind of load variations (e.g. daily, seasonal, etc.) that affect sizing of conventional UFLS stages.

VI. Acknowledgement

This work was funded by the Slovenian Research Agency through the research program Electric Power Systems No. P2-0356 and project Resource management for low latency reliable communications in smart grids—LoLaG, J2-9232. Furthermore, this work was supported by European Regional Development Fund through the OIS-AIR project with the financial support of the ADRION programme.

This work is a subject to a pending International Patent Application No. PCT/EP2018/059048 filled on April 9, 2018.

VII. References

[1] U. Rudez and R. Mihalic, 'RoCoF-based Improvement of Conventional Under-Frequency Load Shedding', in *2019 IEEE Milan PowerTech*, Milan, Italy, Jun. 2019, pp. 1–5, doi: 10.1109/PTC.2019.8810438.

[2] L. Sigrist, L. Rouco, and F. M. Echavarren, 'A review of the state of the art of UFLS schemes for isolated power systems', *Int. J. Electr. Power Energy Syst.*, vol. 99, pp. 525–539, Jul. 2018, doi: 10.1016/j.ijepes.2018.01.052.

[3] L. Sigrist, 'A UFLS Scheme for Small Isolated Power Systems Using Rate-of-Change of Frequency', *IEEE Trans. Power Syst.*, vol. 30, no. 4, pp. 2192–2193, Jul. 2015, doi: 10.1109/TPWRS.2014.2357218.

[4] U. Rudez and R. Mihalic, 'Monitoring the First Frequency Derivative to Improve Adaptive Underfrequency Load-Shedding Schemes', *IEEE Trans. Power Syst.*, vol. 26, no. 2, pp. 839–846, May 2011, doi: 10.1109/TPWRS.2010.2059715.

[5] D. Sodin, R. Ilievska, A. Čampa, M. Smolnikar, and U. Rudez, 'Proving a Concept of Flexible Under-Frequency Load Shedding with Hardware-in-the-Loop Testing', *Energies*, vol. 13, no. 14, p. 3607, Jul. 2020, doi: 10.3390/en13143607.

[6] ENTSO-E, ‘RG CE OH Version 3.1 – Policy 5: Emergency Operations’. Sep. 2017, [Online]. Available: https://eepublicdownloads.entsoe.eu/clean-documents/Publications/SOC/Continental_Europe/oh/170926_Policy_5_ver3_1_43_RGCE_Plenary_approved.pdf.
[7] P. M. Anderson, (Paul M.), A. A. Fouad, and Institute of Electrical and Electronics Engineers, *Power system control and stability*. 2002.